Zeolites

Temperature-Dependent Interconversion of an Anthracene Radical Cation/Electron Moiety to an Electron–Hole Pair in the Pores of Al-ZSM-5 Zeolites**

Hervé Vezin, Alain Moissette, and Claude Brémard*

One of the most intriguing properties of acidic zeolites is their ability to generate organic radical cations spontaneously upon mere sorption of organic molecules.[1] The rigid framework of silicoaluminate porous materials with specific molecular-sieve properties can stabilize radical cations over several months at room temperature. It appears that the presence of heteroatoms such as aluminum in the siliceous framework and a proton as the counterion is a requirement for the efficient stabilization of radical cations. In addition, the tight fit of the radical cation in the pore is also considered to be an important factor for the stabilization of short-lived radical cations.

The characterization of many occluded radical cations is well documented. In contrast, direct evidence of the fate of the ejected electron is rare.[1–3] Typically, the ejected electrons are suggested to be highly delocalized in the zeolite framework. The zeolite framework is also known to contain electron-donor sites capable of transferring electrons to strong acceptors. The nature and structure of the centers responsible for the electron-donating or electron-accepting ability of zeolites is still the subject of controversy and debate.[1,4,5] Understanding the fate of ejected or abstracted electrons may lead to better control in producing high-yielding ionizations. These features have obvious implications in the area of the acid catalysis of hydrocarbons based on zeolites.[1,4,5]

Previously, we have characterized electron–hole pairs stabilized in acidic H_nZSM-5 zeolites loaded with biphenyl.[3] The sorption of biphenyl resulted in spontaneous ionization to give the radical cation and the electron. However, the

[*] Dr. A. Moissette, Dr. C. Brémard
Laboratoire de Spectrochimie Infrarouge et Raman
UMR-CNRS 8516
Centre d'Etudes et de Recherches Lasers et Applications
FR-CNRS 2416, Bât. C5
Université des Sciences et Technologies de Lille
59655 Villeneuve d'Ascq cedex (France)
Fax: (+33) 3-2043-6755
E-mail: alain.moissette@univ-lille1.fr
Dr. H. Vezin
Laboratoire de Chimie Organique et Macromoléculaire
UMR-CNRS 8009, Bât. C4
Université des Sciences et Technologies de Lille
59655 Villeneuve d'Ascq cedex (France)

[**] The authors are very grateful to Dr. J. Patarin for providing ultrapure zeolites. The Centre d'Etudes et de Recherches Lasers et Applications (CERLA) is supported by the Ministère chargé de la recherche, the région Nord/Pas de Calais, and the Fonds Européen de Développement Economique des Régions.

Supporting information for this article is available on the WWW under http://www.angewandte.org or from the author.

 DOI: 10.1002/ange.200352269

system evolved too rapidly to an electron–hole pair to be characterized by pulsed electron paramagnetic resonance (EPR) techniques. In addition, the ionization occurred after activation of zeolites under O_2 at high temperature, and the yield was found to be low.[3] Recently, we have reported the results of investigations by UV/Vis absorption and Raman scattering of the sorption of anthracene (Anth) and parent molecules in H_nZSM-5 dehydrated at moderate temperature.[6] Spontaneous Anth ionization occurs in high yield, and the occluded radical cation $Anth^{+\bullet}$ is found to be stable over several months at room temperature.

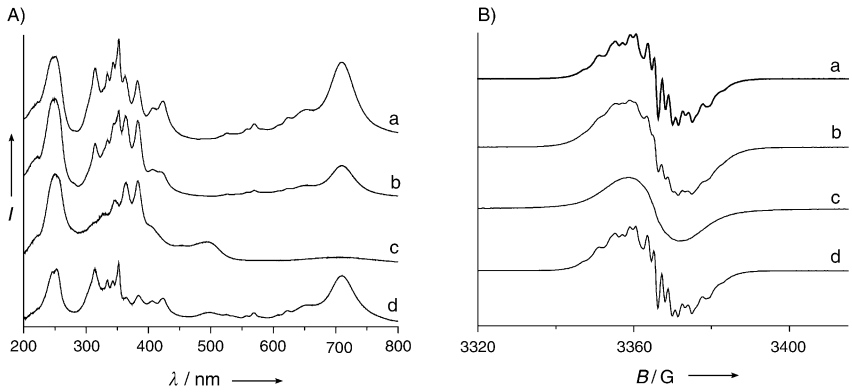

Figure 1. A) Diffuse reflectance UV/Vis spectra for Anth occluded in H_3ZSM-5 at a) room temperature, b) 400 K, c) 473 K, and d) 24 h after cooling to room temperature. Loading: one molecule of Anth per unit cell. B) CW X-band EPR spectra for Anth occluded in H_3ZSM-5 at the same temperatures as in A).

Here, we report the results of EPR and UV/Vis absorption studies of the temperature-dependent reversible conversion of the $Anth^{+\bullet}$/electron moiety to electron–hole pairs in the pores of H_3ZSM-5 zeolite. The emphasis of this paper is set on the characterization of the $Anth^{+\bullet}$/electron moiety and electron–hole pair occluded in the pores of H_3ZSM-5 zeolites by pulsed EPR techniques.

The evacuation of template molecules from the framework of the as-synthesized ZSM-5 zeolite was performed at 773 K under O_2. Subsequent rehydration at room temperature and dehydration at 673 K under Ar provide the porous H_3ZSM-5 material. The comparison of all the physicochemical measurements—powder XRD, ^{29}Si and ^{27}Al MAS-NMR, EPR, Raman, UV/Vis, IR absorption, and chemical analyses—with previous works provides clear evidence of a pure ZSM-5 phase with unit cells of the chemical composition $H_3(AlO_2)_3(SiO_2)_{93}$. In particular, no evidence was found for either extraframework aluminum species or iron(III) impurities.[7,8,9] The framework topology of H_3ZSM-5 is composed of a three-dimensional network of straight and sinusoidal channels. The entrance of the channels is controlled by ten-membered rings of oxygen atoms with dimensions reported as 0.54×0.56 nm^2 for the straight channels and 0.51×0.55 nm^2 for the zigzag ones.[10] The straight channels are sufficiently wide to allow Anth molecules to pass through the openings and to diffuse into the void space.[6]

Bare H_3ZSM-5 zeolite as microcrystals several μm in size was exposed in the dark, under argon, and at room temperature to a weighted amount of dry Anth ($C_{14}H_{10}$). The Anth loading corresponds to one Anth molecule per unit cell of zeolite ($Anth/H_3(AlO_2)_3(SiO_2)_{93}$). The sorption was monitored by diffuse-reflectance UV/Vis absorption (DRUVv), Raman scattering, and continuous-wave (CW)-EPR spectroscopies. The sorption and equilibration were found to be complete after three months at room temperature. The Raman and UV/Vis spectra were found to be typical for $Anth^{+\bullet}$ as the major occluded organic species (spectrum a, Figure 1 A). Nevertheless, no evidence of the ejected electron was obtained with these techniques.[6]

In the CW-EPR spectra recorded after equilibrium at room temperature (spectrum a, Figure 1 B) sharp signals are superimposed over a broad signal of 10 G. No half-field ($g \sim 4$) signal was detected. The double integration of the EPR signal in the $g = 2$ region indicates that the ionization is nearly complete after three months and that it generates spin density corresponding to two unpaired electrons per unit cell. The reference standard sample was obtained by loading 2,2,5,5-tetramethyl-3-pyrrolin-1-yloxy nitroxide radical in ZSM-5 zeolite. The excitation of the complex CW-EPR signal obtained after complete ionization with a two-pulse echo sequence yields a two-spin-process phenomenon. Effectively, in combination with the echo generation, a strong free-induction-decay (FID) process is observed due to the presence of a homogeneous spin packet. These two jointly observed phenomena result from the presence in the sample of two nonequivalent chemical magnetic species.

We performed spin-lattice T_1 measurements using FID inversion recovery with 16-step phase cycling to suppress the echo process and echo inversion recovery and found very long T_1 times for both processes with threefold higher values for the echo process (Figure 2 A). The T_1 values recorded at room temperature were found to be 100 μs and 310 μs for FID and echo processes, respectively. Such behavior gives us the possibility to identify the paramagnetic species responsible for the two distinct spin-magnetic processes.

We recorded two-dimensional spectra for T_1 versus the field sweep for the FID signal and observed along the field direction the typical CW $Anth^{+\bullet}$ spectrum with numerous lines due to the proton hyperfine coupling (Figure 2). The spectrum in Figure 2 A is indicative of the formation of $Anth^{+\bullet}$ in accurate agreement with DRUVv and Raman spectroscopy.[6] This spectrum consists of at least twenty split components. Comparison of these ^{1}H hyperfine splittings with those of a pure $Anth^{+\bullet}$ isotropic spectrum recorded in solution indicates some ^{1}H hyperfine splittings have disappeared due to anisotropic broadening effects. This feature has also previously been observed for $Anth^{+\bullet}$ generated on a silica–alumina catalyst surface and during oxidation by polyoxometalate.[11,12]

Similar experiments with echo detection only yield the observation of the echo shape along the field direction. The

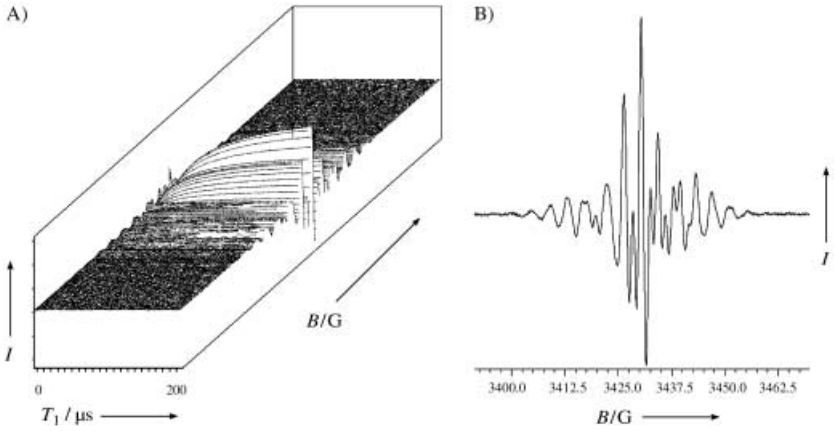

Figure 2. A) 2D spin-lattice relaxation time T_1 versus field-sweep measurements recorded at room temperature for Anth occluded in H_3ZSM-5 relevant to radical cation/electron moiety. The FID inversion recovery with 16-step phase cycling to suppress echo processes was used. B) Projection slice spectrum of pure $Anth^{+\bullet}$ as observed along the field direction.

echo signal is relevant to the electron trapped in the zeolite framework but needs supplementary pulsed EPR experiments.

The differences in T_1 values allow us to characterize separately $Anth^{+\bullet}$ and the trapped electron by spin-echo correlation spectroscopy (SECSY). We performed at room temperature and 4.2 K the analysis of the structure of these two species by using SECSY for the FID (Figure 3A) and echo SECSY for the echo signal (Figure 3B). The SECSY spectra give the usual EPR spectrum along the f_2-axis and the nuclear frequencies along the f_1-axis, respectively. This method provides the distribution of nuclear modulation frequency included in inhomogeneous EPR spectrum. In addition, the characterization of the echo signal was completed by hyperfine sublevel correlation spectroscopy (HYSCORE) experiments (not shown). It has been shown that these HYSCORE experiments offer excellent resolution of the hyperfine splittings.

Firstly, we recorded a 2D SECSY spectrum of the FID process (Figure 3A), and we observe along the diagonal the signature of the proton–electron coupling of $Anth^{+\bullet}$ that was observed on the projection along the CW domain in Figure 2B. Moreover we can observe that the diagonal signal measured at the resonance is not completely symmetric and that on both negative and positive quadrants some cross-peaks appear and occur from Heisenberg spin-exchange mechanisms. This result confirms that an equilibrium should exist between the radical cation and trapped electron.

Secondly, due to the strong FID process, a 16-step phase cycling SECSY sequence was used to suppress completely the anti-echo FID process. The 2D echo SECSY contour plot shows in both positive and negative f_1 quadrants the double-quantum peak ($2\tilde{\nu}(^{13}C) = 7.4$ MHz) of ^{13}C nuclear modulation ($\tilde{\nu}(^{13}C) = 3.7$ MHz) centered at 0 MHz in the f_2 domain (Figure 3B). This is consistent with an unpaired isolated electron coupled with carbon. An additional proton pattern centered at the carbon nuclear frequency is observed with $\nu(^1H) = 14.5$ MHz and combination lines at $2\nu(^1H) = 29$ MHz. Such changes were also observed in the HYSCORE spectrum (not shown) where the ^1H anisotropic constant measured is 9.8 MHz and a weak carbon coupling is observed in the (+,+) f_2 domain with an anisotropic constant of 2.1 MHz and a positive sign for the hyperfine splitting constant. Moreover, no signal features arising from zeolite interactions through ^{29}Si or ^{27}Al were evident in the HYSCORE spectrum. In HYSCORE and SECSY spectra the same patterns are observed at room temperature and at 4.2 K. Due to its quadrupolar moment, the ^{27}Al nucleus can be observed only at 4.2 K. Consequently, the HYSCORE pattern observed at 3.7 MHz at room temperature and at 4.2 K must be attributed to ^{13}C modulation and not to the ^{27}Al nucleus, for which the nuclear modulation frequency is 3.8 MHz. Such results seem to indicate that the electron is trapped in close proximity to the occluded $Anth^{+\bullet}$ radical cation. It should be noted that the trapped electron is stabilized in the zeolite framework with no visible coupling to ^{27}Al or ^{29}Si nuclei and is probably in close proximity to oxygen.

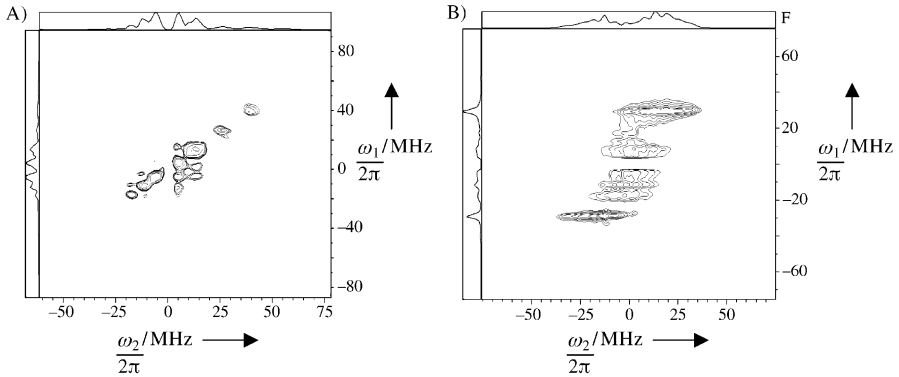

Figure 3. SECSY spectra of Anth occluded in H_3ZSM-5 zeolite relevant to the radical cation/electron moiety. A) Two-pulse FID SECSY spectrum of the radical cation. B) Two-pulse echo SECSY spectrum of the trapped electron. The spectra were recorded at 4.2 K at the maximum of the CW EPR signal. The two-pulse SECSY spectrum was recorded with pulse lengths of 12 ns for $\pi/2$ pulses, and a 16-step phase cycling ($\pi/2-t_1-\pi/2-t_1-t_2-$echo) was applied.

When we heated the sample that had equilibrated at room temperature over three months, the hyperfine structure of the CW spectra disappeared and only a featureless signal was obtained after one hour at 473 K. Double integration of the signals, (spectrum c, Figure 1B) indicates a spin density close to two unpaired electrons per unit cell. The hyperfine splittings reappeared when the sample was cooled to room temperature after an equili-

bration period of several hours (spectrum d, Figure 1 B). An identical phenomenon was observed by DRUVv spectrometry, (Figure 1 A). The intense absorption bands around 300 and 700 nm characteristic of $Anth^{+\cdot}$ disappeared gradually upon heating. This development was complete at 473 K. The resulting spectral maxima (383, 364, 347 nm) were found to be analogous to those exhibited by occluded Anth in the ground state (384, 364, 347 nm) except for a weak and broad-band absorption around 500 nm (spectrum c, Figure 1 A). Both the broad EPR signal and the absorption at 500 nm were straightforwardly attributed to occluded electron–hole pairs with respect to Anth occluded in ground state.

The remanence of the electron–hole pair at room temperature for one hour before the reverse electron-transfer permitted us to perform pulsed EPR investigations. The two-pulse echo experiment recorded for the the so-called electron–hole pair shows the complete disappearance of the FID process in accordance with the disappearance of $Anth^{+\cdot}$. Moreover, T_1 echo measurements yield the same value as that measured for the ejected electron of the $Anth^{+\cdot}$/electron moiety, demonstrating identical relaxation times for the ejected electron and for unpaired electrons involved in the electron–hole pair.

Both the 2D echo SECSY contour plot and the HYSCORE pattern of electron–hole pair were found to be analogous to those recorded for the $Anth^{+\cdot}$/electron moiety. In particular, the 3.7-MHz pattern observed in the HYSCORE spectrum is assigned to ^{13}C nuclei in a straightforward fashion. Such results seem to indicate that the electrons of the electron–hole pairs are in the vicinity of the occluded Anth in ground state. Unfortunately, no evidence was found for coupling between the electrons and the ^{27}Al or ^{29}Si nuclei of the zeolite framework. The electrons of the electron–hole pairs are probably stabilized in the zeolite framework in close proximity to oxygen nuclei. In contrast, coupling between electrons and ^{29}Si and ^{27}Al nuclei was observed previously for the electron–hole pairs stabilized by sorption of biphenyl in $H_3ZSM\text{-}5$.[3] In addition, no half-field signal was detected in the CW spectrum. Thus, there is no evidence for a spin-coupling interaction between the two paramagnetic centers of the electron–hole pair stabilized in the $H_3ZSM\text{-}5$ zeolite loaded with Anth. It should be noted that weak ferromagnetic coupling was previously detected in the electron–hole pair stabilized by biphenyl.[3]

The exposure of solid Anth to the bare zeolite $H_3ZSM\text{-}5$ ($H_3(AlO_2)_3(SiO_2)_{93}$) results in the uptake of Anth molecules at the openings of the pores and diffusion into the straight channels of the zeolite framework. Because of the relatively low ionization potential of Anth in the gas phase (7.44 eV), the electrostatic field in the void space of $H_3ZSM\text{-}5$ suffices to completely ionize Anth, and it is found trapped exclusively as the radical cation [Eq. (1)].

$$Anth + H_3ZSM\text{-}5 \rightarrow Anth^{+\cdot}/H_3ZSM\text{-}5^{-\cdot} \quad (1)$$

The ejected electron was found to be in close proximity to $Anth^{+\cdot}$, and the $Anth^{+\cdot}$/electron moiety was found occluded in the straight channel (Figure 4). However, we found no evidence for the interaction of unpaired electrons with the zeolite nuclei. The $Anth^{+\cdot}/H_3ZSM\text{-}5^{-\cdot}$ moiety exhibits temperature-dependent behavior in agreement with the observation of temperature-dependent electron transfer from the $H_3ZSM\text{-}5$ framework to the $Anth^{+\cdot}$ radical cation through Equation (2).

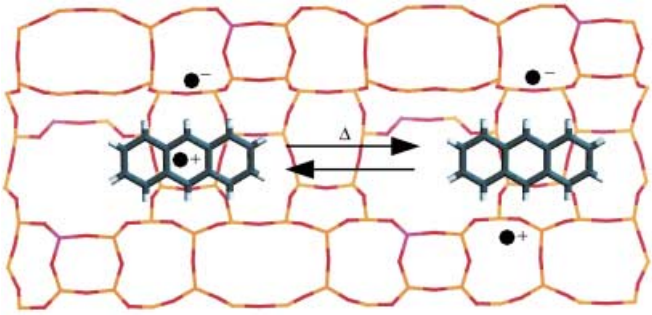

Figure 4. Schematic structures of the $Anth^{+\cdot}$/electron moiety and the electron–hole pair in the straight channel of $H_3ZSM\text{-}5$ zeolite. Yellow, red, and pink sticks represent the Si, O, and Al atoms of zeolite, respectively. Dark gray and white cylinders represent the C and H atoms of anthracene. ● − = trapped electron, ● + = electron-deficient sites in $Anth^{+\cdot}$ and in hole.

$$Anth^{+\cdot}/H_3ZSM\text{-}5^{-\cdot} \overset{\Delta}{\rightleftarrows} Anth/H_3ZSM\text{-}5^{+\cdot -\cdot} \quad (2)$$

The conversion appears to be gradual and fully reversible. In contrast to the behavior of biphenyl in the same zeolite, the spontaneous ionization of Anth and subsequent formation of the electron–hole pair were found to be nearly total. However, no interaction of the unpaired electrons with the zeolite framework was detected. The electron–hole pair appears to be stabilized in high yield in the straight channel of $H_3ZSM\text{-}5$ by anthracene in the ground state in close proximity.

The ability of some porous materials to generate and stabilize electron–hole pairs appears to be the conjunction of intrinsic and complementary properties of both the host and the guest. The process is initiated by the sorption of electron-donor molecules, the shape and size of which are suitable for penetrating the void space of the zeolite.[6] The electrostatic field imposed by the incorporation of Al^{III} and H^+ as the counterion leads to complete ionization. The charge recombination is hampered by the restricted mobility of the sorbed radical cation and efficient electron trapping. The electron capture from the framework by the radical cation rather than direct charge recombination is the most intriguing feature under the confinement of the void space. The long life of the electron–hole pair stabilized by anthracene occluded in $H_3ZSM\text{-}5$ zeolite is attributed to both efficient electron and hole trapping.

Received: July 1, 2003 [Z52269]

Keywords: anthracene · electron transfer · EPR spectroscopy · UV/Vis spectroscopy · zeolites

[1] H. Garcia, H. D. Roth, *Chem. Rev.* **2002**, *102*, 3947 – 4007.
[2] R. I. Samoilova, A. A. Shubin, M. K. Bowman, J. Hüttermann, S. A. Dikanov, *Chem. Phys. Lett.* **2000**, *316*, 404 – 410.
[3] A. Moissette, H. Vezin, I. Gener, J. Patarin, C. Brémard, *Angew. Chem.* **2002**, *114*, 1289 – 1292; *Angew. Chem. Int. Ed.* **2002**, *41*, 1241 – 1244.
[4] I. Kirisci, H. Förster, G. Tasi, J. B. Nagy, *Chem. Rev.* **1999**, *99*, 2085 – 2114.
[5] M. Hunger, J. Weitkamp, *Angew. Chem.* **2001**, *113*, 3040 – 3059; *Angew. Chem. Int. Ed.* **2001**, *40*, 2954 – 2971.
[6] A. Moissette, S. Marquis, I. Gener, C. Brémard, *Phys. Chem. Chem. Phys.* **2002**, *4*, 5690 – 5696.
[7] G. Catana, D. Baetens, T. Mommaerts, R. A. Schoonheydt, B. M. Weckhuysen, *J. Phys. Chem. B* **2001**, *105*, 4904 – 4911.
[8] B. Staudte, A. Gutsze, W. Böhlmann, H. Pfeifer, B. Pichewitz, *Microporous Mesoporous Mater.* **2000**, *40*, 1 – 7.
[9] D. Goldfarb, K. G. Strohmaier, D. E. W. Vaughan, H. Thomann, O. G. Poluektov, J. Schmidt, *J. Am. Chem. Soc.* **1996**, *118*, 4665 – 4671.
[10] H. Van Koningsveld, J. C. Jansen, H. Van Bekkum, *Zeolites* **1990**, *10*, 235 – 242.
[11] G. M. Muha, *J. Phys. Chem.* **1967**, *71*, 640 – 649.
[12] A. M. Khenkin, L. Weiner, Y. Wang, R. Neumann, *J. Am. Chem. Soc.* **2001**, *123*, 8531 – 8542.

